This article was downloaded by: [Renmin University of China]
On: 13 October 2013, At: 10:48
Publisher: Taylor & Francis
Informa Ltd Registered in England and Wales Registered Number: 1072954 Registered office: Mortimer House, 37-41 Mortimer Street, London W1T 3JH, UK

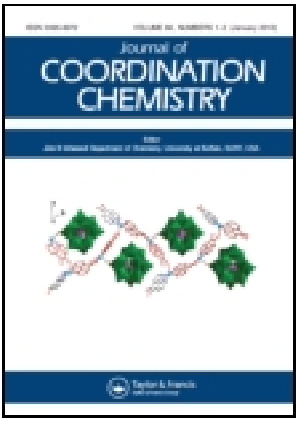

Journal of Coordination Chemistry
Publication details, including instructions for authors and subscription information:
http://www.tandfonline.com/loi/gcoo20

Coordination polymers (Ni^{II} and Co^{II}) based on the rigid bridging ligand, 4,4′-bis(imidazol-1-yl)biphenyl, with (4^6) topology

Wei Zhang [a] & Lujiang Hao [a]

[a] College of Food and Biological Engineering, Shandong Institute of Light Industry , Jinan , PR China

Accepted author version posted online: 22 Apr 2013.Published online: 30 May 2013.

To cite this article: Wei Zhang & Lujiang Hao (2013) Coordination polymers (Ni^{II} and Co^{II}) based on the rigid bridging ligand, 4,4′-bis(imidazol-1-yl)biphenyl, with (4^6) topology, Journal of Coordination Chemistry, 66:12, 2110-2117, DOI: 10.1080/00958972.2013.798653

To link to this article: http://dx.doi.org/10.1080/00958972.2013.798653

PLEASE SCROLL DOWN FOR ARTICLE

Taylor & Francis makes every effort to ensure the accuracy of all the information (the "Content") contained in the publications on our platform. However, Taylor & Francis, our agents, and our licensors make no representations or warranties whatsoever as to the accuracy, completeness, or suitability for any purpose of the Content. Any opinions and views expressed in this publication are the opinions and views of the authors, and are not the views of or endorsed by Taylor & Francis. The accuracy of the Content should not be relied upon and should be independently verified with primary sources of information. Taylor and Francis shall not be liable for any losses, actions, claims, proceedings, demands, costs, expenses, damages, and other liabilities whatsoever or howsoever caused arising directly or indirectly in connection with, in relation to or arising out of the use of the Content.

This article may be used for research, teaching, and private study purposes. Any substantial or systematic reproduction, redistribution, reselling, loan, sub-licensing, systematic supply, or distribution in any form to anyone is expressly forbidden. Terms &

Journal of Coordination Chemistry, 2013
Vol. 66, No. 12, 2110–2117, http://dx.doi.org/10.1080/00958972.2013.798653

Coordination polymers (Ni^{II} and Co^{II}) based on the rigid bridging ligand, 4,4′-bis(imidazol-1-yl)biphenyl, with (4^6) topology

WEI ZHANG and LUJIANG HAO*

College of Food and Biological Engineering, Shandong Institute of Light Industry,
Jinan, PR China

(*Received 6 October 2012; in final form 6 February 2013*)

Two coordination polymers, $\{[Ni_{0.5}(4,4'\text{-bib})Cl][(4,4'\text{-bib})_{0.5}]\cdot H_2O\}_n$ (**1**) and $\{[Co(4,4'\text{-bib})_3(H_2O)_2][NO_3]_2\cdot H_2O\}_n$ (**2**) (4,4′-bib = 4,4′-bis(imidazol-1-yl)biphenyl) have been hydrothermally synthesized. Their structures have been determined by single-crystal X-ray diffraction analyses and are further characterized by elemental analyses, IR, thermogravimetric analyses, and powder X-ray diffraction. In **1**, each Ni^{II} is linked by four μ_{2-4},4′-bib ligands in 2-D (4,4)-networks, which are further connected through host–guest interaction to form a 3-D packing diagram with 1-D channels. In **2**, each Co^{II} is linked by two μ_{2-4},4′-bib and two μ_{1-4},4′-bib ligands in a 1-D zigzag chain, further connected through non-covalent interactions (including O–H···N, O–H···O, C–H···π, and π···π interactions) to form a 3-D supramolecular structure. 4,4′-bib exhibits μ_2-, μ_1-, and μ_0-coordination during the construction of **1** and **2**. From the topological view, the overall structures of **1** and **2** possess (4^6) topology.

Keywords: 4,4′-Bis(imidazol-1-yl)biphenyl; Nickel; Cobalt

1. Introduction

The synthesis of metal coordination polymers (CPs) has interest for topological novelty and application as functional materials [1–6]. Many metal CPs have been synthesized. Yet, the goal of predicting crystal structures remains a long-term challenge [7–9].

Generally, CPs are constructed from transitional metal ions and organic acid or base under suitable reaction environments, such as pH, solvent, templates, temperatures, etc. [10–15]. Ligands are selected by an enormous amount of research to synthesize CPs with unique structure and functions, especially for imidazole-containing ligands, such as 1,4-di(1-imidazolyl) benzene, 1-(1-imidazolyl)-4-(imidazol-1-ylmethyl)benzene, 1,3,5-tris(1-imidazolyl) benzene, 1,3,5-tris(imidazole-1-ylmethyl)-2,4,6-trimethylbenzene, 4,4′-bis(imidazol-1-yl)-biphenyl, 1-(1-imidazolyl)-3,5-bis(imidazol-1-ylmethyl) benzene, etc. [9, 16, 17, 18–22]. Imidazole-containing ligands build polynuclear species, acting as bridging, chelating, and charge balance ligands [23–28].

Taking inspiration from the aforementioned points, we hydrothermally synthesized two CPs based on 4,4′-bis(imidazol-1-yl)biphenyl (4,4′-bib), $\{[Ni_{0.5}(4,4'\text{-bib})Cl][(4,4'\text{-bib})_{0.5}]\cdot$

---

*Corresponding author. Email: lujiang_hao@163.com

$H_2O\}_n$ (**1**) and $\{[Co(4,4'\text{-bib})_3(H_2O)_2][NO_3]_2\cdot H_2O\}_n$ (**2**). X-ray diffraction analyses reveal that 4,4′-bib exhibits μ_2-, μ_1-, and μ_0-coordination in **1** and **2**. In **1**, each Ni^{II} is linked by four μ_{2-4},4′-bib in 2-D (4,4)-networks, which are further connected through host–guest interactions to form a 3-D packing diagram with 1-D channels. In **2**, each Co^{II} is linked by two μ_{2-4},4′-bib and two μ_{1-4},4′-bib to form 1-D zigzag chains, which are further connected through non-covalent interactions (including O–H···N, O–H···O, C–H···π, and π···π interactions) to form a 3-D supramolecular structure.

2. Experimental

2.1. *Materials and methods*

4,4′-Bis(imidazol-1-yl)biphenyl was commercially available. Elemental analyses (C, N, and H) were performed on an EA1110 CHNS-0 CE elemental analyzer. IR (KBr pellet) spectra were recorded on a Nicolet Magna 750FT-IR spectrometer. Thermogravimetric measurements were carried out in a nitrogen stream using a Netzsch STA449C apparatus with a heating rate of 10 °C min^{-1}. Powder X-ray diffraction (PXRD) patterns were measured on a Shimadzu XRD-6000 X-ray diffractometer with Cu-Kα ($\lambda = 1.5418$ Å) radiation at room temperature.

2.2. *Synthesis*

2.2.1. Synthesis of $\{[Ni_{0.5}(4,4'\text{-bib})Cl][(4,4'\text{-bib})_{0.5}]\cdot H_2O\}_n$ (1). The synthesis of **1** is performed in a 25 mL teflon-lined stainless steel vessel. A mixture of 4,4′-bib (0.20 mM, 0.059 g), terphenyl-2,5,2′,5′-tetracarboxylic acid (0.10 mM, 0.034 g), nickel chloride hexahydrate (0.20 mM, 0.047 g), NaOH (0.30 mM, 0.012 g), and 12 mL H_2O was heated to 170 °C for 3 days followed by slow cooling (10 °C/h) to room temperature, giving green block crystals. Yield of 51% (based on Ni). Anal. (%) Calcd for $C_{54}H_{50}Cl_2N_{12}NiO_2$ (1028.65): C, 63.05; H, 4.90; N, 16.34%. Found: C, 62.96; H, 4.11; N, 16.13%. IR (KBr pellet, cm^{-1}): 3258(m), 3096(m), 1607(w), 1517(s), 1417(w), 1319(s), 1134(s), 957(m), 827(m), 751(m), 637(m), and 516(w).

2.2.2. Synthesis of $\{[Co(4,4'\text{-bib})_3(H_2O)_2][NO_3]_2\cdot H_2O\}_n$ (2). **2** is synthesized in a 25 mL teflon-lined stainless steel vessel. A mixture of 4,4′-bib (0.20 mM, 0.042 g), 5-(4-pyridyl)isophthalic acid (0.20 mM, 0.049 g), cobalt nitrate hexahydrate (0.40 mM, 0.116 g), NaOH (0.30 mM, 0.012 g), and 12 mL H_2O was heated to 170 °C for 3 days, followed by slow cooling (10 °C/h) to room temperature giving red needle crystals. Yield of 59% (based on Co). Anal. (%) Calcd for $C_{54}H_{48}CoN_{14}O_9$ (1095.98): C, 59.18; H, 4.41; N, 17.89%. Found: C, 58.67; H, 5.07; N, 17.41%. IR (KBr pellet, cm^{-1}): 3136(m), 2375(w), 1613(m), 1511(s), 1389(m), 1302(s), 1067(m), 969(m), 831(m), 761(m), 644(m), and 531(m).

2.3. *X-ray crystallography*

Intensity data collection was carried out on a Siemens SMART diffractometer equipped with a CCD detector using Mo-Kα monochromated radiation ($\lambda = 0.71073$ Å) at 293(2) K.

Absorption corrections were based on multiple and symmetry-equivalent reflections in the data-set using SADABS based on the method of blessing. The structures were solved by direct methods and refined by full-matrix least-squares using SHELXTL [29, 30]. Crystallographic data for **1** and **2** are given in table 1. Selected bond lengths and angles are listed in table 2.

3. Results and discussion

3.1. *Structure description of* $\{[Ni_{0.5}(4,4'\text{-bib})Cl][(4,4'\text{-bib})_{0.5}]\cdot H_2O\}_n$ (**1**)

Single-crystal X-ray analysis reveals that **1** crystallizes in the monoclinic system, *P*2(1)/*c* space group. As shown in figure 1, there are a half of a crystallographically independent Ni^{II}, one 4,4′-bib as the bridging group, one coordinated Cl^-, a half of 4,4′-bib as guest molecules, and one free water in the asymmetric unit of **1**. Each Ni^{II} is six-coordinate by four N from four 4,4′-bib ligands [Ni(1)–N(1) = 2.125(1), Ni(1)–N(4) = 2.102(3) å] and two Cl^- [Ni(1)–Cl(1) = 2.117(3) å], showing a distorted octahedral coordination geometry.

The 4,4′-bib in **1** are linkers and guest molecules. A 4,4′-bib bridge connects two neighboring Ni^{II} ions forming a 2-D (4,4) net with a much bigger diamond (17.625 × 17.625 Å) (figure 2). A 3-D framework was constructed via interaction of host skeletons $[Ni(4,4'\text{-bib})_2Cl_2]_n$ and guest 4,4′-bib (figure 3). From the topological point of view, all Ni^{II} ions are 4-connecting nodes and the shortest circuit is a six-membered ring. So the 2-D sheet can be simplified to a 4-connected topology with a point symbol of 4^4 net. Taking into consideration the host–guest interaction, the 3-D supramolecule can be regarded as a 6-connected topology with a point symbol of 4^6-dia net.

Table 1. Crystallographic data and details of diffraction experiments for **1** and **2**.

	1	**2**
Formula	$C_{54}H_{50}Cl_2N_{12}NiO_2$	$C_{54}H_{48}CoN_{14}O_9$
M_r	1028.65	1095.99
Crystal system	Monoclinic	Monoclinic
Space group	P2(1)/c	P2(1)/c
a (Å)	17.377(4)	8.982(3)
b (Å)	12.752(1)	29.908(1)
c (Å)	11.689(4)	19.619(6)
α (°)	90.00	90.00
β (°)	108.999(0)	94.362(6)
γ (°)	90.00	90.00
V (Å^3)	2449(2)	5255(3)
Z	2	4
ρ (g cm^{-3})	1.445	1.385
μ (mm^{-1})	0.667	0.398
T (K)	296(2)	293(2)
R_{int}	0.0245	0.1658
R [$I > 2\sigma(I)$]	$R_1 = 0.0674$ $wR_2 = 0.1959$	$R_1 = 0.0784$ $wR_2 = 0.2135$
R (all data)	$R_1 = 0.0706$ $wR_2 = 0.1415$	$R_1 = 0.1206$ $wR_2 = 0.1588$
Goof	0.999	1.000

[a] $R_1 = \Sigma||F_{obsd.}| - |F_{calcd}||/\Sigma|F_{obsd.}|$. [b] $wR_2 = \sum[w(F^2_{obsd.} - F^2_{calcd})^2]/\sum[w(F^2_{obsd.})^2]^{1/2}$. $w = 1/[\sigma^2(F_o^2) + xP + (yP)^2]$; with $P = (F_o^2 + 2F_c^2)/3$, [c] goof $= [\sum w(F^2_{obsd.} - F^2_{calcd})^2/(n-p)]^{1/2}$, where n = number of reflections, p = parameter used.

Table 2. Selected bond lengths (Å) and angles (°) for **1** and **2**^{a}.

Complex ***1***							
Ni(1)–Cl(1)	2.117(3)	N(1)–Ni(1)	2.125(3)	N(4)–Ni(1)$^{\#2}$	2.102(3)	Ni(1)–N(4)$^{\#3}$	2.102(3)
Ni(1)–N(4)$^{\#4}$	2.102(3)	Ni(1)–Cl(1)$^{\#5}$	2.117(3)	Ni(1)–N(1)$^{\#5}$	2.125(3)		
N(4)$^{\#3}$–Ni(1)–N(4)$^{\#4}$	180.00(13)	N(4)$^{\#3}$–Ni(1)–Cl(1)$^{\#5}$	89.79(11)	N(4)$^{\#4}$–Ni(1)–Cl(1)$^{\#5}$	90.21(11)	N(4)$^{\#3}$–Ni(1)–Cl(1)	90.21(11)
N(4)$^{\#4}$–Ni(1)–Cl(1)	89.79(11)	Cl(1)$^{\#5}$–Ni(1)–Cl(1)	180.000(1)	N(4)$^{\#3}$–Ni(1)–N(1)$^{\#5}$	87.71(11)	N(4)$^{\#4}$–Ni(1)–N(1)$^{\#5}$	92.29(11)
Cl(1)$^{\#5}$–Ni(1)–N(1)$^{\#5}$	89.87(11)	Cl(1)–Ni(1)–N(1)$^{\#5}$	90.13(11)	N(4)$^{\#3}$–Ni(1)–N(1)	92.29(11)	N(4)$^{\#4}$–Ni(1)–N(1)	87.71(11)
Cl(1)$^{\#5}$–Ni(1)–N(1)	90.13(11)	Cl(1)–Ni(1)–N(1)	89.87(11)	N(1)$^{\#5}$–Ni(1)–N(1)	180.00(17)		
Symmetry codes: #1 $-x, -y+1, -z$; #2 $-x, y+1/2, -z+1/2$; #3 $-x, y-1/2, -z+1/2$; #4 $x+1, -y+3/2, z+1/2$; #5 $-x+1, -y+1, -z+1$.							
Complex ***2***							
Co(1)–N(5)	2.153(3)	Co(1)–N(11)$^{\#1}$	2.143(3)	Co(1)–O(1 W)	2.1501(14)	Co(1)–N(9)	2.155(3)
Co(1)–N(1)	2.157(3)	Co(1)–O(2 W)	2.1582(15)	N(11)–Co(1)$^{\#2}$	2.143(3)		
N(5)–Co(1)–N(11)$^{\#1}$	92.12(10)	N(5)–Co(1)–O(1 W)	88.93(8)	N(11)$^{\#1}$–Co(1)–O(1 W)	92.41(9)	N(5)–Co(1)–N(9)	90.30(10)
N(11)$^{\#1}$–Co(1)–N(9)	90.51(11)	O(1 W)–Co(1)–N(9)	177.01(8)	N(5)–Co(1)–N(1)	176.32(10)	N(11)$^{\#1}$–Co(1)–N(1)	90.82(10)
O(1 W)–Co(1)–N(1)	88.73(8)	N(9)–Co(1)–N(1)	91.89(10)	N(5)–Co(1)–O(2 W)	88.40(8)	N(11)$^{\#1}$–Co(1)–O(2 W)	176.47(8)
O(1 W)–Co(1)–O(2 W)	84.12(6)	N(9)–Co(1)–O(2 W)	92.97(9)	N(1)–Co(1)–O(2 W)	88.53(8)		
Symmetry codes: #1 $-x+3, y-1/2, -z+1/2$; #2 $-x+3, y+1/2, -z+1/2$.							

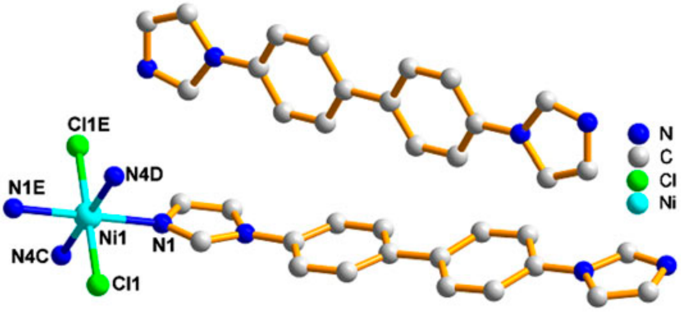

Figure 1. Coordination environment of Ni^{II} in **1**. Hydrogens are omitted for clarity. Symmetry codes: A: $-x$, $1-y$, $-z$; B: $-x$, $0.5+y$, $0.5-z$; C: $1+x$, $1.5-y$, $0.5+z$; D: $-x$, $-0.5+y$, $0.5-z$; E: $1-x$, $1-y$, $1-z$.

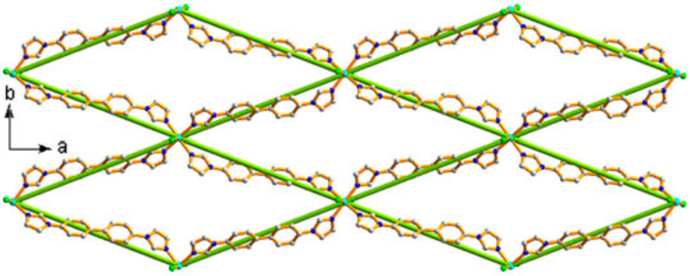

Figure 2. The 2-D (4,4) networks of **1** viewed along the ab plane.

3.2. *Structure description of* $\{[Co(4,4'\text{-}bib)_3(H_2O)_2][NO_3]_2\cdot H_2O\}_n$ (**2**)

Single-crystal X-ray analysis reveals that **2** crystallizes in the monoclinic system, P2(1)/c space group. As shown in figure 4, there are one crystallographically independent Co^{II}, one bridging and two terminal 4,4′-bib ligands, two coordinated waters, two nitrates, and one free water in the asymmetric unit of **2**. Each Co^{II} is six-coordinate by four N from two bridging and two terminal 4,4′-bib [Co(1)–N(1) = 2.157(1), Co(1)–N(5) = 2.153(2), Co

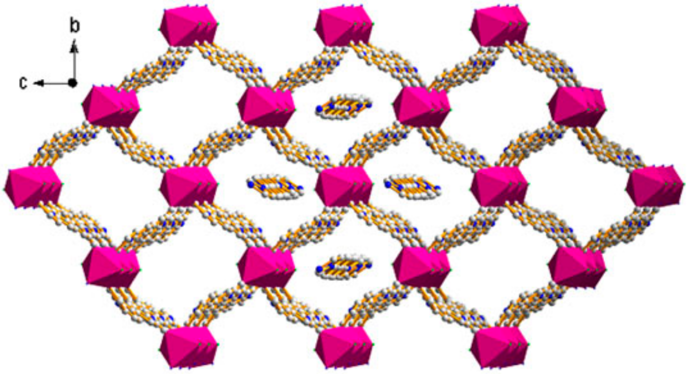

Figure 3. The 3-D frameworks of **1** viewed along the bc plane (partly fulfilled guest molecules).

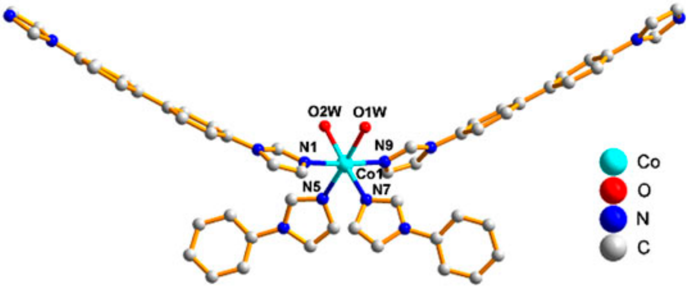

Figure 4. Coordination environment of Co^{II} in **2**. Hydrogens are omitted for clarity. Symmetry codes: A: $3-x$, $0.5+y$, $0.5-z$; B: $3-x$, $-0.5+y$, $0.5-z$.

(1)–N(7) = 2.155(2), and Co(1)–N(9) = 2.162(5) Å] and two coordinated waters [Co(1)–O (1w) = 2.150(1), Co(1)–O(2w) = 2.158(2) Å] showing a distorted octahedral coordination geometry.

The 4,4′-bib in **2** exhibits μ_2- and μ_1- coordination. Each Co^{II} is linked by two μ_{2-4},4′-bib forming the wave-like chain. Each Co^{II} is further coordinated by two μ_{1-4},4′-bib to saturate the coordination geometry like the two long wings of a dragonfly (figure 5). The resulting chains are cross-linked via hydrogen-bond interactions [O2 W–H4 W···N8 = 2.783(6), O2 W–H3 W···O6 = 3.033(3), and O1 W–H2 W···N4 = 2.778(5) å], C–H···π interactions between neighboring chains [C33–H33···π = 3.867 å] and π···π interactions between 4,4′-bib from one 1-D zigzag chain and another 4,4′-bib from another 1-D chain with center-to-center distance of 4.138 Å leading to a 3-D supramolecular architecture (figure 6). From the topological point of view, the overall structure of **2** can also be defined as a 6-connected network with the Schläfli symbol of 4^6.

Although **1** and **2** were both constructed from 4,4′-bib and related transition metals under similar reaction conditions, a large difference between the architectures results from the different coordination modes, μ_2- and μ_0- in **1**, and μ_2- and μ_1- in **2**. Compared with previously reported bisimidazole complexes, the successful characterizations of **1** and **2** proved that 4,4′-bib is an effective bridging ligand and guest molecule [31–33].

3.3. *IR spectra*

IR spectra of **1** and **2** are similar, which can be seen in figure S1. Absorption bands of 3000–3300 cm^{-1} in **1** and **2** can be attributed to characteristic peaks of water O–H vibrations. Vibrations at 1610 and 1355 cm^{-1} correspond to asymmetric and symmetric stretches of carboxylates of 4,4′-bib, respectively.

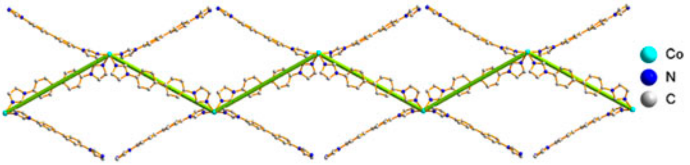

Figure 5. The 1-D zigzag chain of **2**.

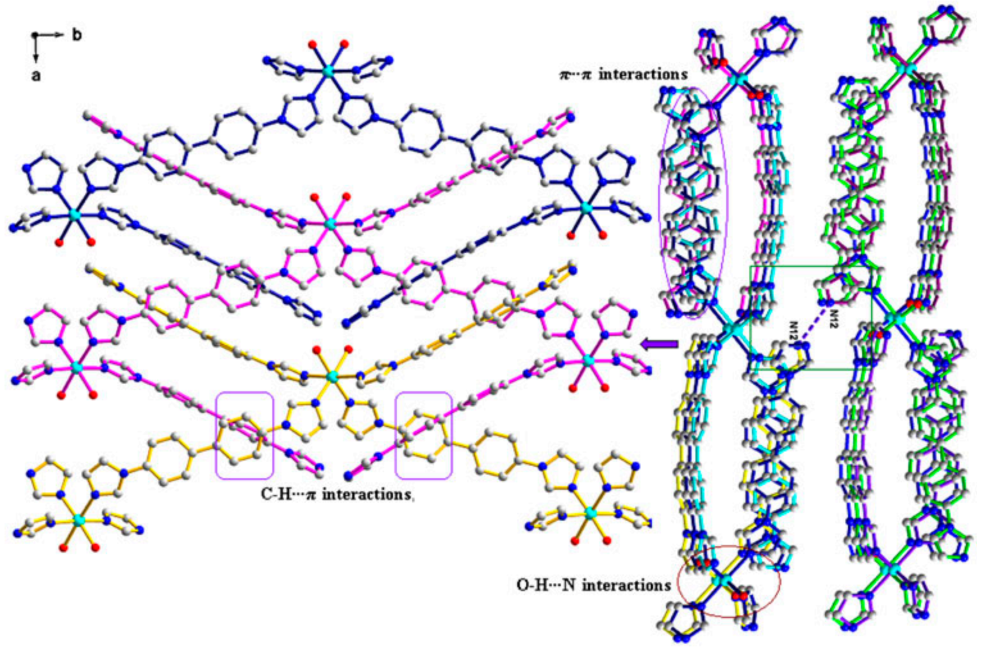

Figure 6. The 2-D networks constructed with intersecting 1-D zigzag chains viewed along the ab plane (left) and 3-D frameworks (right) based on non-covalent interactions in **2**.

3.4. *PXRD and TGA analysis*

In order to check the phase purity of these complexes, PXRD patterns of **1** and **2** were checked at room temperature. As shown in figure S2, the peak positions of the simulated and experimental PXRD patterns are in agreement demonstrating phase purity of complexes. The dissimilarities in intensity may be due to the preferred orientation of crystalline powder samples.

Thermogravimetric analysis (TGA) measurements were carried out on a Perkin-Elmer Diamond TG/DTA instrument with a flow of dry air and a heating rate of 5 °C/min from room temperature to 1000 °C. As shown in figure S3, TGA curve indicates that **1** and **2** are unstable with increasing temperature. Complex **1** shows a weight loss of 3.67% from 80–130 °C corresponding to the release of free water (Calcd 3.50%); weight loss of 14.57% at 250 °C corresponds to release of guest bib (Calcd 14.02%) and decomposition of the residue occurred at 340 °C. The residual weight is ca. 7.53% (Calcd for NiO: 7.26%). For **2**, a weight loss of 5.31% was observed at 170 °C, corresponding to loss of coordinated water (Calcd 4.93%), and further weight loss was observed at 370 °C. The residual weight is ca. 7.83% (Calcd for Co_2O_3: 7.57%).

4. Conclusion

We have developed a synthetic strategy for CPs by employing 4,4′-bis(imidazol-1-yl)-biphenyl as the N-donor. Further systematic studies for design and synthesis of crystalline materials with 4,4′-bib and other building blocks are underway in our laboratory.

Supplementary material

For **1** and **2**, further details on the crystal structure investigations may be obtained from the Cambridge Crystallographic Data Center, CCDC, 12 Union Road, Cambridge CB2 1EZ, UK [Telephone: +44-(0)1223-762-910; Fax: +44-(0)1223-336-033; E-mail: deposit@ccdc.cam.ac.uk; http://www.ccdc.cam.ac.uk/deposit] on quoting the depository number CCDC-904728 for **1**, 904729 for **2.**

Acknowledgments

The work was supported by Natural Science Foundation of Shandong Province (ZR2012CM019).

References

[1] S. Qiu, G. Zhu. *Coord. Chem. Rev.*, **253**, 2891 (2009).
[2] M. O'Keeffe, O.M. Yaghi. *Chem. Rev.*, **112**, 675 (2012).
[3] D. Sun, G.G. Luo, N. Zhang, R.B. Huang, L.S. Zheng. *Chem. Commun.*, **47**, 1461 (2011).
[4] L. Hou, J.P.H. Deng, C.J. Doonan, H. Furukawa, R.B. Ferreira, J. Towne, C.B. Knobler, B. Wang, O.M. Yaghi. *Science*, **327**, 846 (2010).
[5] X.L. Yang, M.H. Xie, C. Zou, Y.B. He, B.L. Chen, M. O'Keeffe, C.D. Wu. *J. Am. Chem. Soc.*, **134**, 10638 (2012).
[6] S. Kitagawa, R. Kitaura, S. Noro. *Angew. Chem. Int. Ed.*, **43**, 2334 (2004).
[7] L.M. Fan, X.T. Zhang, D.C. Li, D. Sun, W. Zhang, J.M. Dou. *Cryst. Eng. Commun.*, **15**, 349 (2013).
[8] L.F. Ma, Y.Y. Wang, L.Y. Wang, D.H. Lu, S.R. Batten, J.G. Wang. *Cryst. Growth Des.*, **9**, 2036 (2009).
[9] Z.X. Li, J.P. Zhao, E.C. Sanudo, H. Ma, Z.D. Pan, Y.F. Zeng, X.H. Bu. *Inorg. Chem.*, **48**, 11601 (2009).
[10] Y.Z. Zheng, M.L. Tong, W. Xue, W.X. Zhang, X.M. Chen, F. Grandjean, G.J. Long. *Angew. Chem. Int. Ed.*, **46**, 6076 (2007).
[11] X.T. Zhang, L.M. Fan, Z. Sun, W. Zhang, D.C. Li, J.M. Dou, L. Han. *Cryst. Growth Des.*, **13**, 792 (2013).
[12] X.T. Zhang, L.M. Fan, X. Zhao, D. Sun, D.C. Li, J.M. Dou. *Cryst. Eng. Commun.*, **14**, 2053 (2012).
[13] D. Sun, Y.H. Li, H.J. Hao, F.J. Liu, Y.M. Wen, R.B. Huang, L.S. Zheng. *Cryst. Growth Des.*, **11**, 3323 (2011).
[14] L.M. Fan, D.C. Li, P.H. Wei, P.Q. Tang, M.H. Li, D. Yuan, G.Z. Liu, X.T. Zhang, J.M. Dou. *J. Coord. Chem.*, **64**, 3031 (2011).
[15] S.N. Wang, R.R. Yun, Y.Q. Peng, Q.F. Zhang, J. Lu, J.M. Dou, J.F. Bai, D.C. Li, D.Q. Wang. *Cryst. Growth Des.*, **12**, 79 (2012).
[16] X.T. Zhang, L.M. Fan, Z. Sun, W. Zhang, D.C. Li, P.H. Wei, B. Li, G.Z. Liu, J.M. Dou. *Chinese J. Inorg. Chem.*, **28**, 1809 (2012).
[17] L. Chen, G.J. Xu, K.Z. Shao, Y.H. Zhao, G.S. Yang, Y.Q. Lan, X.L. Wang, H.B. Xu, Z.M. Su. *Cryst. Eng. Commun.*, **12**, 2157 (2010).
[18] S.Y. Zhang, S.J. Yang, Y.R. Tang, Y. Xue, J.S. You. *J. Am. Chem. Soc.*, **131**, 1689 (2009).
[19] Z. Su, J. Fan, T. Okamura, M.S. Chen, S.S. Chen, W.Y. Sun, N. Ueyama. *Cryst. Growth Des.*, **10**, 1911 (2010).
[20] C.C. Ji, J. Li, Y.Z. Li, Z.J. Guo, H.G. Zheng. *Cryst. Eng. Commun.*, **13**, 459 (2011).
[21] X.T. Zhang, D. Sun, B. Li, L.M. Fan, B. Li, P.H. Wei. *Cryst. Growth Des.*, **12**, 3845 (2012).
[22] Z. Sun, L.M. Fan, W. Zhang, D.C. Li, P.H. Wei, B. Li, G.Z. Liu, L.J. Tian, X.T. Zhang. *J. Coord. Chem.*, **65**, 1847 (2012).
[23] L.L. Wen, F. Wang, J. Feng, K.L. Lv, C.G. Wang, D.F. Li. *Cryst. Growth Des.*, **9**, 3581 (2009).
[24] L. Chen, G.J. Xu, K.Z. Shao, Y.H. Zhao, G.S. Yang, Y.Q. Lan, X.L. Wang, H.B. Xu, Z.M. Su. *CrystEngComm*, **12**, 2157 (2010).
[25] T.T. Hou, S.M. Yue, X.R. Yue, J.F. Ma. *J. Coord. Chem.*, **65**, 3895 (2012).
[26] X.T. Zhang, L.M. Fan, Z. Sun, W. Zhang, D.C. Li, P.H. Wei, B. Li, J.M. Dou. *J. Coord. Chem.*, **65**, 3205 (2012).
[27] L.L. Wen, J.B. Zhao, K.L. Lv, K.J. Deng, X.K. Leng, D.F. Li. *Cryst. Growth Des.*, **12**, 1603 (2012).
[28] J.B. Lin, J.P. Zhang, X.M. Chen. *J. Am. Chem. Soc.*, **132**, 6654 (2010).
[29] Bruker. *SMART and SAINT*, Madison, WI (2007).
[30] G.M. Sheldrick. *Acta Cryst.*, **A64**, 112 (2008).
[31] S.W. Jin, D.Q. Wang, Y.C. Xu. *J. Coord. Chem.*, **65**, 1953 (2012).
[32] S.X. Yan, D. Zhao, T. Li, R. Wang, X.R. Meng. *J. Coord. Chem.*, **65**, 945 (2012).
[33] M. Pi, T. Wang, C.M. Jin. *J. Coord. Chem.*, **64**, 600 (2011).